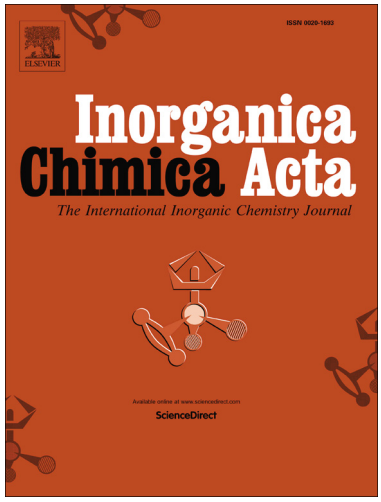

Research paper

Base metal Schiff base complexes applied as catalysts for the oxidation of *n*-octane

Ebrahim Kadwa, Holger B. Friedrich, Muhammad D. Bala

PII: S0020-1693(16)30913-6
DOI: http://dx.doi.org/10.1016/j.ica.2017.04.032
Reference: ICA 17537

To appear in: *Inorganica Chimica Acta*

Received Date: 18 November 2016
Revised Date: 6 March 2017
Accepted Date: 18 April 2017

Please cite this article as: E. Kadwa, H.B. Friedrich, M.D. Bala, Base metal Schiff base complexes applied as catalysts for the oxidation of *n*-octane, *Inorganica Chimica Acta* (2017), doi: http://dx.doi.org/10.1016/j.ica.2017.04.032

Base metal Schiff base complexes applied as catalysts for the oxidation of *n*-octane

Ebrahim Kadwa, Holger B. Friedrich and Muhammad D. Bala*

School of Chemistry and Physics, University of KwaZulu-Natal, Private Bag X54001, Durban 4000, South Africa

Abstract

The catalytic oxidation of *n*-octane to value-added oxygenates has been studied with a series of salen-type complexes of iron. The four iron Schiff base complexes *N*,*N'*-*bis*(salicylidene)-L-iron(III) chloride [L = 1,2-phenylenediamine (**5**); ethylenediamine (**6**); propylenediamine (**7**) and butylenediamine (**8**)] were synthesised by variation of the bridging diamine backbone. All the complexes are fully characterised and the crystal structure of **7** is for the first time reported as a centrosymmetric dimer observed to crystallise in the triclinic $P\bar{1}$ system. The application of **5**-**8** in this oxidation reaction represents a rare example of the systematic use of iron-salen complexes for the liquid-phase functionalisation of $C_{sp}{}^3$–H bonds of straight chain alkanes. All catalysts displayed activity with H_2O_2 and TBHP as oxidants that resulted in a mixture of oxygenated products dominated by the ketones (2-, 3- and 4-octanones). Observed trends and variations in catalytic activities of the complexes is related to differences in chemical/structural features and changes in reaction conditions. A detailed analysis of selectivity parameters of the complexes to the variety of oxygenates is also presented and rationalised.

Keywords: *Paraffin functionalisation; Schiff base; Iron complexes; Regioselectivity parameter*

*Correspondence to: e-mail- bala@ukzn.ac.za; fax- +27 31 260 3091

1. Introduction

The functionalisation of linear (*n*-) alkanes under mild conditions is notoriously difficult and has been the subject of much research effort [1-3]. The holy-grail of linear alkane activation and oxidation [4] is the cytochrome P450 enzyme which contains a heme group, a complex containing iron tetra-coordinated in the plane of a porphyrin ring via four N-donors at the active site [5]. Salen-type ligands are often used as cytochrome P450 active site mimics as they share certain similarities with porphyrins: N-donor groups, a formal charge of (2-), tetra-coordination to the metal with the metal coordinated in a plane formed by the N- and O-donor groups. Additionally, some salen-type complexes have been shown to reversibly bind dioxygen (O_2). Hence, the catalytic oxidation of many organic substrates has been accomplished with salen-type complexes of Mn, Co, V, Cr, Ti and other metals [6-12]. The general popularity of salen-type Schiff base ligands as "heme mimics" in oxidation catalysis is due to their ease of synthesis, availability of starting materials at a relatively low cost, the large range of possible variants with different substituents and the possibility of their coordination to, and stabilisation of, most metal centres [13].

Although iron complexes of salen-type ligands are well known [14-19], there exists a general paucity of reports on their use as alkane oxidation catalysts and to the best of our knowledge, the nearest catalytic application to this report is the use of an FeSalenCl complex for the oxidation of amino acids [20] cyclohexane [21], various alkenes and chalcones [7], certain organic dyes [22, 23], sulphides and sulphoxides [9] and phenol derivatives [24]. And for the purpose of close mimicry to heme in the design of the supporting architecture around the ONNO donor atoms of the salen ligand, research has proven that variation in the rigidity/flexibility and functionality of the backbone atoms has more general influence on the behaviour of a coordinated metal than variation of the substituents on the bridging phenyl rings [25]. Hence, in this study we have varied the backbone architecture of the four salen-type ligands and their corresponding complexes and used iron as the basis of the catalyst design to further benefit from advantages that include reversible redox behaviour, low cost, earth abundance, ready availability and low toxicity [26]. Therefore, as a continuation of our studies on paraffin activation [3, 27] we report the first application of cheap iron centred Schiff base complexes as biomimetic catalysts for the oxidation of *n*-octane to value added oxygenated products, including terminal products such as 1-octanal.

2. Results and discussion

2.1. Synthesis of complexes

Scheme 1 represents a general synthetic route to the four iron Schiff base complexes. Full characterisation details for all the ligands (**1**-**4**) have previously been published [27]. All the metal complexes (**5**-**8)** are paramagnetic, however, they were unambiguously characterised by their sharp melting points, exact CHN elemental analysis, IR, HRMS and for **7** single crystal XRD.

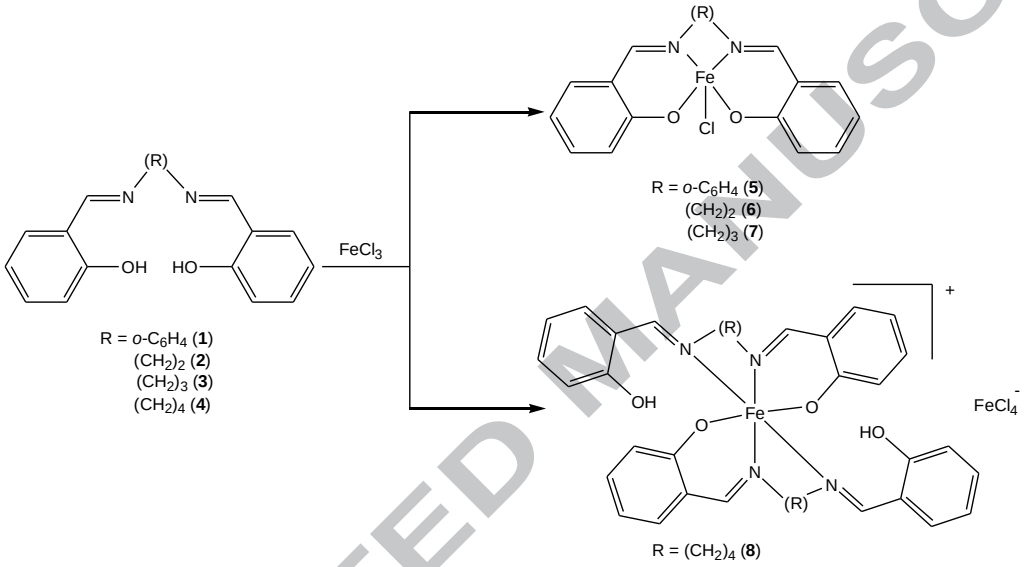

Scheme 1. Route to the synthesis of iron Schiff base complexes **5**-**8**.

2.2. IR Spectroscopy

Selected peaks from the IR spectra of ligands and complexes are presented in Table 1. Also shown are the peak frequency shifts upon complexation.

Table 1. Comparison of infrared frequencies of selected functional groups of compounds **1**-**8**.

Ligand vs complex	**imine C=N / cm^{-1}**	**phenolic C-O / cm^{-1}**	**phenyl C=C / cm^{-1}**	**phenyl C-H / cm^{-1}**
1 salophen	1613	1277	1481	761
5 FesalophenCl	1604	1315	1461	760

Shift*	-9	+38	-20	-1
2 salen	1636	1284	1498	742
6 FesalenCl	1618	1303	1445	758
Shift*	-18	+19	-53	+6
3 salpn	1637	1282	1499	753
7 FesalpnCl	1611	1301	1472	757
Shift*	-26	+19	-27	+4
4 salbn	1633	1285	1498	753
8 Fe(salbn)$_2$FeCl$_4$	1661	1285	1476	760
Shift*	+28	0	-22	+7

* Shift = (freq. complex - freq. ligand)

One of the most important observations from the data in Table 1 is the weakening (shift to lower wavenumbers) of the imine C=N bond upon complexation to the metal, implying there is loss of some double bond character as the pi electrons are delocalised in the metallocycle. This weakening is proportional to the length of the ligand backbone (phenylene weakens the least, followed by ethylene and then propylene) except for the butylene backbone. In the case of the butylene backbone, IR data suggest that complexation strengthens the C=N bond. A possible explanation for this may be ascribed to the increased degrees of rotational freedom due to the multiple conformation possibilities for the very flexible four carbon chain of the backbone leading to the imine-Fe-imine bonds being more linear. This high flexibility of the backbone may be responsible for the difficulty we encountered on the attempted isolation of quality single crystals of complex **8**. Also noted from the IR data is the general strengthening (shift to higher wavenumbers) of the phenolic C-O bond upon complexation to Fe and subsequent formation of the O-Fe-O bonds. For the complexation of salbn (**4**) to yield Fe(salbn)$_2$FeCl$_4$ (**8**), the peak at 1285 cm^{-1} remained unchanged (due to the uncoordinated phenolic C-O), with a poorly resolved shoulder at circa 1300 cm^{-1}, attributed to the coordinated C-O functionality in the complex. In general, there is an overall shift in the peak positions of the significant functional groups upon complexation of respective ligands to Fe.

The cyclometallated moieties that form upon complexation impart stability to the metal complexes formed.

2.3. X-Ray Crystallography

The molecular structure of complex **7** FesalpnCl was determined by X-ray diffraction analysis of its single crystal data, while those of **5** and **6** we isolated and determined, exactly matched previously reported [15, 28] results and are henceforth excluded from this discussion except where necessary for the purpose of comparison. However, the molecular structure of complex **8** is yet to be reported by single crystal XRD due probably to the high flexibility of the six membered butylene diamine backbone which in comparison to the other complexes has a higher degree of freedom that often leads to disorder, distortion and poor quality of diffraction data. An ORTEP representation of the arrangement and connectivity of atoms in complex **7** is presented in Fig 1.

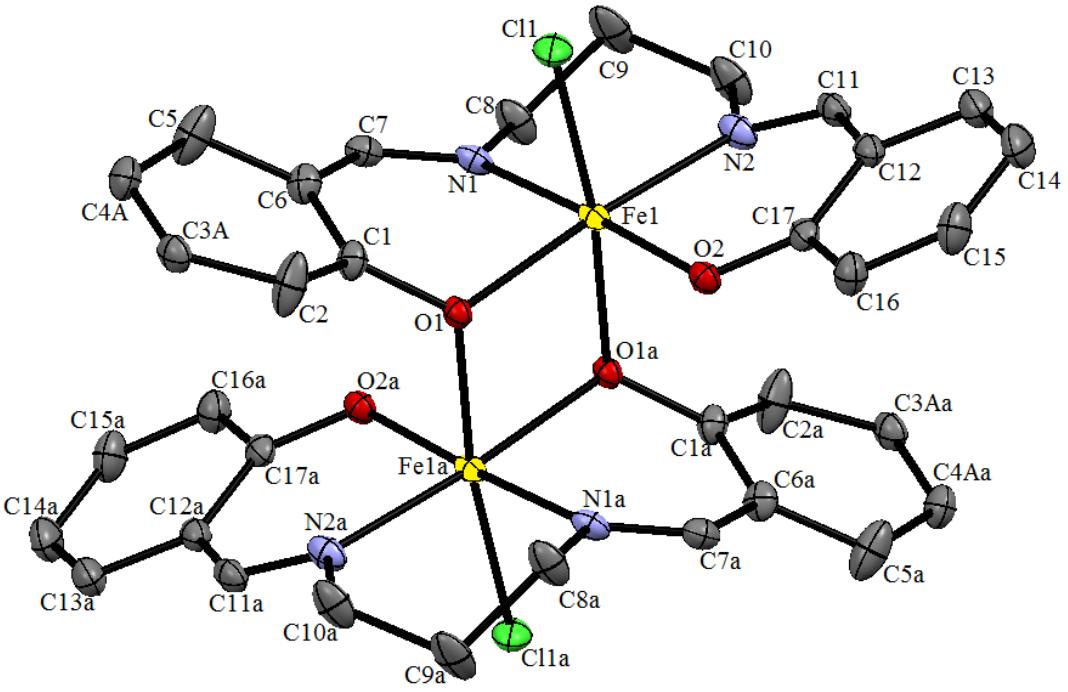

Figure 1. *ORTEP* diagram of **7** with thermal ellipsoids drawn at the 50% probability level. Hydrogen atoms and a second, poorly resolved dimer are omitted for clarity. Selected bond lengths (Å) and angles (°) **Fe1-N1,** 2.145 (2); **Fe1-N2,** 2.152 (2); **Fe1-O1,** 2.0241 (17); **Fe1-O2,** 1.9030 (17); **Fe1-Cl1,** 2.3309 (11); **Fe1-O1a,** 2.1136 (17); **N1-Fe-N2,** 91.32 (8); **O1-Fe-O2,** 95.74 (7); **N1-Fe-O1,** 84.26 (7); **N2-Fe-O2,** 87.89 (8); **Cl-Fe-O1,** 96.16 (6); **Cl-Fe-O2,** 94.59 (6); **Cl-Fe-N1,** 90.61 (6); **Cl-Fe-N2,** 92.44 (7).

Amongst the earliest structural data determinations of salen-type Schiff base complexes to be published are those of **5** and **6**, which were previously reported by Elmali *et al.* [28] and Gerloch and Mabbs [15]. Related structures have been published for (ferrous and ferric) iron complexes of **3**, which contain axial ligands other than a chloride, often with additional substituents on the ligand [29-32], but the crystal structure obtained for **7** is new. However, no crystal structure of complex **8** was found from a survey of current literature. The asymmetric unit of complex **7** crystallised as dimeric species in the centrosymmetric triclinic $P\bar{1}$ system, similar to that reported for complex **6**. The Fe-O-Fe molecular dimers occurred through the sharing of one oxygen atom from each ligand between two iron nuclei. The two types of Fe-O bonds that resulted (Fe1-O1 and Fe1-O1a), are non-equivalent with the dimer-forming bonds (Fe1-O1a) being longer than the normal phenolic (Fe1-O1) bonds due primarily to the effects of the two connected Fe centres. Each iron centre in the dimeric crystal of **7** is hexa-coordinated in an octahedral environment that is situated approximately 0.54 Å away from the basal plane defined by the donor ONNO atoms which, due to non-equivalent axes, show rhombic distortions of the octahedral planes [33]. When compared with related previously reported counterparts (**5** and **6**), the distortions were less pronounced in **7** than in **6** as flexibility of the propylene backbone is greater than that of the ethylene backbone, and the bond angle formed between the nitrogen donors and the iron centre (N-Fe-N) increased with an increase in the carbon chain length and flexibility of the ligand backbone.

2.4. Catalytic conversion of the substrate *n*-octane using peroxide based oxidants

The type, accessibility and cost of the oxidant (source of oxygen) is very important in oxidation catalysis. Air and molecular oxygen are the preferred sources of oxygen, but for highly unreactive substrates such as alkanes, activated oxidants, mostly peroxides, are often employed. In this study we have employed hydrogen peroxide (H_2O_2) and tertiary butyl hydroperoxide (TBHP), which are common peroxide-based oxidants, for the oxidation of the substrate *n*-octane under catalytic conditions with the isolated complexes **5-8** as catalysts. The result presented in Figure 2 indicates that a blank reaction (in the absence of any added catalyst) with H_2O_2 as the oxidant displayed a very low conversion, while use of catalysts with this oxidant led to significantly improved total conversions. The homogeneous catalysts (**5-8)** were all catalytically active in the conversion of *n*-octane to oxygenates and complex **6** with the tightest carbon backbone architecture was the least active in this catalytic process.

An increase in the length of the alkyl backbone from an ethylene (**6**) to a propylene (**7**) group afforded greater catalytic activity, while a longer butylene (**8**) group did not impart any additional advantage to the catalytic activity, remaining at circa 10% conversion. About 4% conversion of the substrate with the more stable TBHP oxidant occurred even in the absence of an added catalyst. However, increased activities were observed with the use of the catalysts. In summary, all the complexes **5-8** were active for the activation of the substrate and a direct correlation relating catalytic activity with the variation in ligand backbone is observed (Fig. 2). The general trend in catalytic activity could directly be linked to the hydrophobicity of the ligand backbone. Where reactivity increased with an increase in the alkyl chain length (for catalysts **6-8**) or possession of an aromatic group (for the higher reactivity of catalyst **5**). In previous studies with monooxygenase enzymes like cytochrome P-450 and other biomimetic catalysts for paraffin activation, it was established that the hydrophobic regions of the catalysts enabled the ready uptake, correct orientation, and hydroxylation of C-H bonds [34]. Other related homogeneous systems have obtained similar conversions with H_2O_2 [35] and higher conversions with TBHP [3, 36].

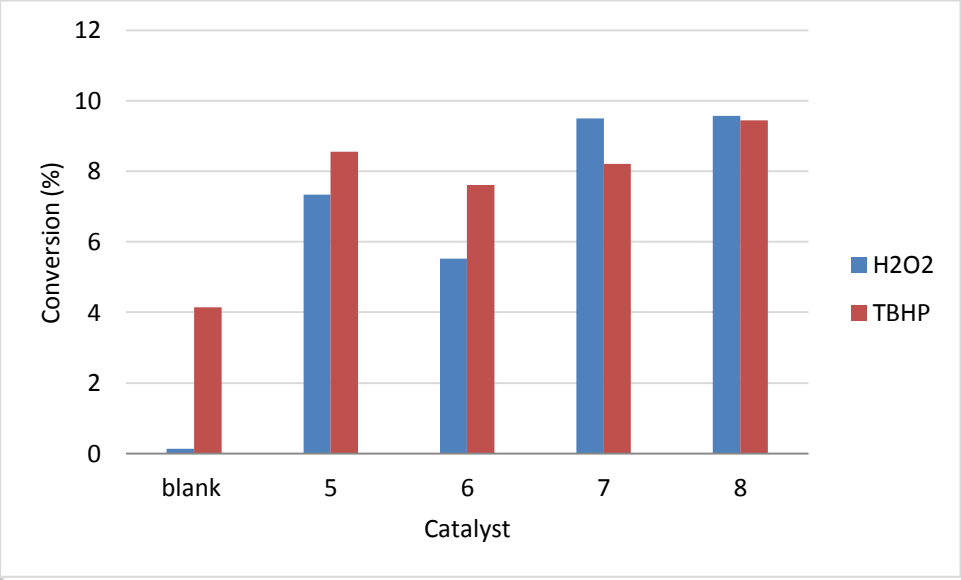

Figure 2. Catalytic conversion of *n*-octane by complexes **5-8** using H_2O_2 and TBHP as oxidants.

2.5. Product selectivity and analysis of the regioselectivity parameter

Statistically, depending on the position of attack and extent of oxidation, a total of nine oxygenated products (octanols, octanal, octanones and octanoic acid) are possible for the functionalisation of *n*-octane with an atom of oxygen. These are the six products of internal carbon activation (4-, 3-, and 2- octanols and octanones) and three of terminal carbon activation (1-octanol, octanal and octanoic acid- the only product that requires the addition of two oxygen atoms). A combination of these in the product stream creates a selectivity difficulty which is to date the greatest challenge of paraffin activation. Thus the need is to develop new catalysts capable of maintaining a lean distribution of preferably the three products of terminal carbon activation. Hence, the concept of the regioselectivity parameter has become useful in paraffin activation as a means to express catalyst efficiency and selectivity or product distribution. The regioselectivity parameter for *n*-octane (C1:C2:C3:C4) is the relative reactivity at carbon positions 1, 2, 3, 4 respectively along its backbone and is used to analyse selectivity to the highlighted plethora of products possible in the oxidation reaction data. It represents the relative reactivity of the internal methylene (CH_2) hydrogen atoms normalised to the terminal methyl (CH_3) hydrogen atoms at carbon position 1. Products were grouped together based on the position of the inserted oxygen, with normalisation carried out by dividing the total selectivity at each carbon by the number of hydrogens at that position (three for the terminal CH_3 and two for each unique internal CH_2). As a reference point, the reactivity at the terminal carbon 1 was set to one. For this study, the selectivity data expressed in terms of the various product groups and the selectivity parameter expressing total reactivity at each carbon atom are presented in Table 2.

Table 2. Product distribution in the oxidation of *n*-octane catalysed by catalysts **5-8**.

Oxidant	**H_2O_2**					**TBHP**				
	Product distribution (%)					**Product distribution (%)**				
Catalyst	**-one (4-;3-;2-)**	**-nol (4-;3-;2-;1-)**	**-nal**	**Acid**	**Regioselectivity parameter* C1 : C2 : C3 : C4**	**-one (4-;3-;2-)**	**-nol (4-;3-;2-;1-)**	**-nal**	**Acid**	**Regioselectivity parameter* C1 : C2 : C3 : C4**
Blank	100 (29; 36; 35)	0	0	0	**0.0 : 1.2 : 1.3 : 1.0**	74 (21; 24; 28)	13 (3; 0; 4; 5)	3	10	**1.0 : 2.5 : 2.0 : 2.0**
5	54 (16; 20; 18)	36 (8; 2; 9; 16)	10	0	**1.0 : 1.5 : 1.3 : 1.4**	78 (23; 26; 29)	12 (4; 0; 5; 3)	3	7	**1.0 : 3.9 : 3.0 : 3.1**
6	62 (19; 23; 21)	25 (8; 1; 8; 7)	10	3	**1.0 : 2.2 : 1.8 : 2.0**	74 (21; 24; 29)	15 (4; 3; 5; 4)	2	9	**1.0 : 3.3 : 2.7 : 2.5**
7	54 (17; 19; 18)	35 (8; 0; 7; 20)	8	4	**1.0 : 1.2 : 0.9 : 1.2**	72 (21; 23; 29)	18 (3; 8; 4; 3)	0	9	**1.0 : 3.8 : 3.7 : 2.9**

8	53 (16; 18; 19)	34 (8; 1; 7; 18)	8	4	**1.0 : 1.3 : 0.9 : 1.2**	76 (22; 24; 29)	15 (4; 2; 4; 4)	0	1 0	**1.0 : 3.8 : 3.0 : 2.9**

Conditions for all entries: 5 ml MeCN, catalyst: n-octane: oxidant = 1: 50: 150 (mol/mol), 80 °C, 48h, stirred at 100 rpm. * = Regioselectivity parameter (C1:C2:C3:C4) is the relative reactivity at carbon positions 1, 2, 3 and 4 respectively on the *n*-octane backbone. Reactivity at C1 is normalised to 1.0.

Previous reports of regioselectivity on the oxidative functionalisation of *n*-alkanes have been published for *n*-hexane, *n*-heptane, *n*-octane and *n*-decane where it was generally established that differences in competitive functionalisation at the terminal and internal C-H bonds has led to two distinct regioselectivity possibilities. On the one hand, zero terminal C-H selectivity may lead to the observance of only products of internal C-H activation (mainly ketones). This scenario has been observed for systems using: an iron-based metal-organic framework (MOF) catalyst, [37] a titanium-doped silicate catalyst, [38] an osmium-based catalyst with an iron-based promoter [39] and, a salen-type manganese complex immobilised onto a polymer membrane support [40]. Thermal oxidation of *n*-octane in the liquid phase with oxygen as the oxidant also resulted exclusively in the functionalisation of internal carbons, except when cracking of a C-C bond resulted in two carboxylic acids [41]. On the other hand, even when functionalisation does occur at the terminal primary C-H bonds, reactivity at each of the possible internal C-H bonds is always higher leading to more ketones and secondary alcohols, as observed for the oxidation of *n*-octane with a bimetallic MOF-5 catalyst containing iron and zinc [42] and a biphasic water/ionic liquid catalyst system [35]. We have observed reactivity at the terminal and internal C-H bonds. The C1:C2:C3:C4 ratio is very low, most notably using catalysts **7** and **8** with H_2O_2 where the ratio 1:1:1:1 obtained is the most even product distribution at carbon atoms of *n*-octane reported to date.

In agreement with some of the findings and established trends highlighted above, this study also indicates that the dominant product groups identified with H_2O_2 and TBHP as oxidants are the ketones comprising over 50 and 70% product selectivity respectively. Analysis of the regioselectivity profiles for selectivity to more desired terminal products (1-octanol, octanal and octanoic acid) indicates that H_2O_2 as oxidant yielded statistically more terminal C-H activation with reasonable amounts of, especially, octanal observed with all the catalysts at up to 10% conversion. This is an interesting observation that might serve as a technique for the oxidation of an existing primary alcohol to the aldehyde [43]. In addition, trace amounts of octanoic acid were observed with all the catalysts and all four alcohols were typically produced with 1-octanol as the dominant product. Similar selectivity profiles were obtained for 2- and 4-octanol, while the catalysts were usually least selective towards 3-octanol. This

contrasts with the selectivity to ketones where 3-octanone was the most prevalent, possibly indicating that further oxidation from octanol to octanone is more facile at the C3 position. In general, unlike the overall catalyst activity, the selectivity to oxygenated products was observed to be independent of the ligand backbone.

2.6. Catalyst deactivation and nature of the active intermediate

The colour of the solution changed from dark red to yellow as the reaction proceeded. After 48 h a light orange solid precipitated out of the solution. This was washed with diethyl ether, dried and analysed by IR (ATR). The IR spectrum of the isolated species contained OH peaks indicating the presence of iron hydroxo species. We were unable to perform any further analysis on the recovered species due to its absolute insolubility. UV analysis of the reaction mixture showed that the complex changed in solution upon addition of H_2O_2. This change was due to H_2O_2 and not as a result of *n*-octane (heating the complex with only *n*-octane added did not alter the pattern of its UV spectrum). A UV/vis time dependent monitoring of the reaction mixture showed that the absorbance peak at 470 nm which is due to the ligand to metal ($PhO^- \rightarrow Fe^{3+}$) charge transfer (LMCT) transition decreased in intensity as the reaction progressed, which is in agreement with earlier observations [9]. Thence we propose high-valent iron-salen oxo specie $[Fe^{IV}=O(salen)]^{+\cdot}$ as the active intermediate in this study. Formation of the active specie occurs via an oxidative reaction of the complex with H_2O_2 in solution. This specie has been studied and characterised by others [44, 45] using a variety of spectroscopic techniques and its function as a medium for the transfer of oxygen to the substrate is widely accepted [9, 20, 23, 46]. Relating this to the observed product distribution (*vide supra*) clearly indicates that the formation of octyl hydroxo compounds was the initial step in the oxidation of *n*-octane to the variety of products (octanols, octanones and octanoic acid) observed in this study.

3. Conclusions

Catalysts based on a combination of cheap ligands (Schiff bases) and environmentally friendly metal (Fe) have been employed for the activation of highly unreactive $C_{sp}{}^3$–H bonds of *n*-octane. In comparison to related results for homogeneous paraffin oxidation, the catalysts used in this study showed improved product distribution in favour of terminal carbon (C1) functionalisation utilising a simple H_2O_2 oxidant. Thus there is a regioselectivity advantage for the use of these catalyst systems in the direct oxidation of *n*-octane to industrially useful terminal products such as 1-octanal and octanoic acid.

4. Experimental

4.1. Ligand synthesis

All the four ligands *N*,*N'*-bis(salicylidene)-1,2-phenylenediamine (**1**, salophen), *N*,*N'*-bis(salicylidene)ethylenediamine (**2**, salen), *N*,*N'*-bis(salicylidene)propylenediamine (**3**, salpn) and *N*,*N'*-bis(salicylidene)butylenediamine (**4**, salbn) were synthesised by established methods we reported earlier [27].

4.2. Synthesis of iron complexes

General procedure for the synthesis of the complexes: A suspension of $FeCl_3$ (*ca*. 15 mmol) in 50 mL of ethanol was added dropwise to a hot (*ca*. 50 °C) solution of ligand (ca. 12 mmol) in 50 mL of ethanol, which was kept stirring in a round bottomed flask. An immediate colour change from orange/yellow to dark red/purple was observed. A reflux condenser was then attached to the round bottomed flask and the reaction was maintained at reflux overnight. After cooling to room temperature, the precipitated complex was filtered off, washed with ice-cold ethanol and dried in air.

FesalophenCl (**5**): Red powder, yield = 72 %, m.p. = 347-350 °C. Selected IR peak frequencies (cm^{-1}): 1604 (C=N), 1315 (C=O), 1461 and 760. m/z = 370.0399, corresponding to [**5**-Cl]$^+$. Analysis found (calculated) for $C_{20}H_{14}N_2O_2FeCl$ (%): C, 58.53 (59.22); H, 3.13 (3.48); N, 6.98 (6.91).

FesalenCl (**6**): Red powder, yield = 76 %, m.p. = 257-263 °C. Selected IR peak frequencies (cm^{-1}): 1618 (C=N), 1303 (C=O), 1445 and 758. m/z = 322.0398, corresponding to [**6**-Cl]$^+$. Analysis found (calculated) for $C_{16}H_{14}N_2O_2FeCl$ (%): C, 53.44 (53.74); H, 3.44 (3.95); N, 8.16 (7.83).

FesalpnCl (**7**): Red powder, yield = 54 %, m.p. = 202-205 °C. Selected IR peak frequencies (cm^{-1}): 1611 (C=N), 1301 (C=O), 1472 and 757.m/z = 336.0555, corresponding to [**7**-Cl]$^+$. Analysis found (calculated) for $C_{17}H_{16}N_2O_2FeCl$ (%): C, 54.86 (54.94); H, 4.34 (4.34); N, 6.53 (7.54).

$Fe(salbn)_2FeCl_4$ (**8**): Dark purple powder, yield = 69 %, m.p. = 237-238 °C. m/z = 646.2252, corresponding to [**8**-$FeCl_4$]$^+$. Selected IR peak frequencies (cm^{-1}): 1661 (C=N), 1285 (C=O), 1476 and 760. Analysis found (calculated) for $C_{36}H_{38}N_4O_4Fe_2Cl_2.6H_2O$ (%): C, 44.92 (45.40); H, 4.40 (5.29); N, 5.56 (5.88).

4.3. Catalytic testing for the oxidation of n-*octane*

The catalysts **5-8** were tested for activity in the oxidation of *n*-octane in the presence of tert-butyl hydroperoxide (TBHP) and hydrogen peroxide (H_2O_2) as oxidants. Reactions were carried out in batches in 25 mL round bottom flasks fitted with condensers and sealed at the top to prevent loss of any volatilised *n*-octane. In a typical reaction, a catalyst (0.01 g) was weighed into the flask and solvent (5 mL acetonitrile (MeCN)) was added using a pipette. Catalyst, substrate and oxidant were added in that order in the (molar) ratio 1:50:150, respectively. Pentanoic acid (ca. 0.008 g, weighed accurately) was used as the internal standard. Reactions were stirred (100 rpm) at 80 °C for 48 h. Conditions were kept constant to allow for comparison of the various catalysts and oxidants. At the end of each catalytic run, the reaction vessel was allowed to cool to room temperature. Duplicate samples were removed from the reaction vessel and analysed by GC using the single point internal standard method.

*4.4. X-ray structure collection, solution and refinement on complex **7***

A single crystal of complex **7** with dimensions 0.23 x 0.15 x 0.08 mm^{-3} was selected and glued on to the tip of a glass fibre. The crystal was then mounted in a stream of cold nitrogen at 100(1) K and centred in the X-ray beam by using a video camera. The crystal evaluation and data collection were performed on a Bruker APEXII diffractometer with Mo Kα (λ = 0.71073 Å) radiation and diffractometer to crystal distance of 4.00 cm. The initial cell matrix was obtained from three series of scans at different starting angles. Each series consisted of 12 frames collected at intervals of 0.5º in a 6º range about with the exposure time of 10 seconds per frame. The reflections were successfully indexed by an automated indexing routine built in the APEXII program suite [47]. The final cell constants were calculated from a set of 6460 strong reflections from the actual data collection. The data were collected by using the full sphere data collection routine to survey the reciprocal space to the extent of a full sphere to a resolution of 0.75 Å. A total of 7866 data were harvested by collecting 2216 frames at intervals of 0.5º scans in ω and φ with exposure times of 15 sec per frame. These highly redundant datasets were corrected for Lorentz and polarization effects. The absorption correction was based on fitting a function to the empirical transmission surface as sampled by multiple equivalent measurements [47]. The systematic absences in the diffraction data were uniquely consistent for the space group $P\bar{1}$ that yielded chemically reasonable and computationally stable results of refinement [48]. A successful solution by the direct methods

of SIR97 [49] provided all non-hydrogen atoms from the E-map. All non-hydrogen atoms were refined with anisotropic displacement coefficients. All hydrogen atoms were included in the structure factor calculation at idealized positions and were allowed to ride on the neighbouring atoms with relative isotropic displacement coefficients. The final least-squares refinement of 567 parameters against 7866 data resulted in residuals R (based on F^2 for $I \geq 2\sigma$) and wR (based on F^2 for all data) of 0.0409 and 0.1106, respectively. The final difference Fourier map was featureless. The molecular diagram is drawn with 50% probability ellipsoids.

Crystallographic data for the structure of complex **7** has been deposited with the Cambridge Crystallographic Data Centre, CCDC 1507900. The data can be obtained free of charge at http://www.ccdc.cam.ac.uk/conts/retrieving.html (or from the Cambridge Crystallographic Data Centre, 12 Union Road Cambridge CB2 1EZ, UK; Fax: +44-1223/336-033; E-mail: deposit@ccdc.cam.ac.uk).

Acknowledgements

We are grateful for financial grants from the Department of Science and Technology-National Research Foundation (DST-NRF) Centre of Excellence in Catalysis (c* change, grants for PAR06 and PAR08). We also thank Dr Bernard Owaga for crystal data collection and analysis.

References

[1] A.E. Shilov, G.B. Shul'pin, Chem. Rev. 97 (1997) 2879-2932.
[2] L.S. Shul'pina, A.R. Kudinov, D. Mandelli, W.A. Carvalho, Y.N. Kozlov, M.M. Vinogradov, N.S. Ikonnikov, G.B. Shul'pin, J. Organomet. Chem. 793 (2015) 217-231.
[3] L. Soobramoney, M.D. Bala, H.B. Friedrich, DTr 43 (2014) 15968-15978.
[4] I.G. Denisov, T.M. Makris, S.G. Sligar, I. Schlichting, Chem. Rev. 105 (2005) 2253-2278.
[5] IUPAC, Compendium of chemical terminology 2ed., Blackwell Scientific Publications, Oxford, 1997.
[6] T. Punniyamurthy, S. Velusamy, J. Iqbal, Chem. Rev. 105 (2005) 2329-2364.
[7] A. Dhakshinamoorthy, K. Pitchumani, Tetrahedron 62 (2006) 9911-9918.
[8] V. Mirkhani, M. Moghadam, S. Tangestaninejad, B. Bahramian, Applied Catalysis A: General 313 (2006) 122-129.
[9] A.M.I. Jayaseeli, S. Rajagopal, J. Mol. Catal. A: Chem. 309 (2009) 103-110.
[10] L. Canali, D.C. Sherrington, Chem. Soc. Rev. 28 (1999) 85-93.
[11] E.N. Jacobsen, Comprehensive Organometallic Chemistry, 2 ed., Pergamon, New York, 1995.
[12] T. Katsuki, J. Mol. Catal. A: Chem. 113 (1996) 87-107.
[13] N.S. Venkataramanan, G. Kuppuraj, S. Rajagopal, Coord. Chem. Rev. 249 (2005) 1249-1268.
[14] P. Pfeiffer, E. Breith, E. Lübbe, T. Tsumaki, Justus Liebigs Ann. Chem. 503 (1933) 84-130.

[15] M. Gerloch, F.E. Mabbs, Journal of the Chemical Society A: Inorganic, Physical, Theoretical (1967) 1900-1908.
[16] M. Gerloch, F.E. Mabbs, Journal of the Chemical Society A: Inorganic, Physical, Theoretical (1967) 1598-1608.
[17] J.L.K.F. de Vries, J.M. Trooster, E. de Boer, Journal of the Chemical Society D: Chemical Communications (1970) 604-605.
[18] J.L.K.F. de Vries, J.M. Trooster, E. de Boer, J. Chem. Soc., Dalton Trans. (1974) 1771-1777.
[19] A. Earnshaw, E.A. King, L.F. Larkworthy, Journal of the Chemical Society A: Inorganic, Physical, Theoretical (1968) 1048-1052.
[20] S. Góger, D. Bogáth, G. Baráth, A.J. Simaan, G. Speier, J. Kaizer, J. Inorg. Biochem. 123 (2013) 46-52.
[21] G.C. Salomão, M.H.N. Olsen, V. Drago, C. Fernandes, L. Cardozo Filho, O.A.C. Antunes, Catal. Commun. 8 (2007) 69-72.
[22] S. Gazi, A. Rajakumar, N.D.P. Singh, J. Hazard. Mater. 183 (2010) 894-901.
[23] C. Bai, W. Xiao, D. Feng, M. Xian, D. Guo, Z. Ge, Y. Zhou, Chem. Eng. J. 215–216 (2013) 227-234.
[24] R. Ikeda, H. Tanaka, H. Uyama, S. Kobayashi, Poly 43 (2002) 3475-3481.
[25] R.H. Holm, J. Am. Chem. Soc. 82 (1960) 5632-5636.
[26] A. Böttcher, E.R. Birnbaum, M.W. Day, H.B. Gray, M.W. Grinstaff, J.A. Labinger, J. Mol. Catal. A: Chem. 117 (1997) 229-242.
[27] E. Kadwa, M.D. Bala, H.B. Friedrich, Applied Clay Science 95 (2014) 340-347.
[28] A. Elmali, Y. Elerman, I. Svoboda, F. H., AcCrC 49 (1993) 1365-1367.
[29] J.C. Fanning, X. Wang, A.E. Koziol, G.J. Palenik, Inorg. Chim. Acta 232 (1995) 199-201.
[30] Z.-L. You, H.-L. Zhu, W.-S. Liu, Acta Crystallographica Section E 60 (2004) m794-m796.
[31] Y. Yahsi, H. Kara, L. Sorace, O. Buyukgungor, Inorg. Chim. Acta 366 (2011) 191-197.
[32] S. Dutta, P. Biswas, J. Mol. Struct. 996 (2011) 31-37.
[33] F.A. Cotton, Basic Inorganic Chemistry, John Wiley and Sons, Singapore, 1995.
[34] A. Wada, S. Ogo, S. Nagatomo, T. Kitagawa, Y. Watanabe, K. Jitsukawa, H. Masuda, Inorg. Chem. 41 (2002) 616-618.
[35] S.G. Mncube, M.D. Bala, J. Mol. Liq. 215 (2016) 396-401.
[36] D. Naicker, H.B. Friedrich, B. Omondi, RSC Advances 5 (2015) 63123-63129.
[37] A. Dhakshinamoorthy, M. Alvaro, H. Garcia, Chemistry – A European Journal 17 (2011) 6256-6262.
[38] R.H.P.R. Poladi, C.C. Landry, Microporous Mesoporous Mater. 52 (2002) 11-18.
[39] S.-M. Yiu, W.-L. Man, T.-C. Lau, J. Am. Chem. Soc. 130 (2008) 10821-10827.
[40] T.C.O. MacLeod, M.V. Kirillova, A.J.L. Pombeiro, M.A. Schiavon, M.D. Assis, Applied Catalysis A: General 372 (2010) 191-198.
[41] F. Garcia-Ochoa, A. Romero, J. Querol, Ind. Eng. Chem. Res. 28 (1989) 43-48.
[42] M.N. Cele, H.B. Friedrich, M.D. Bala, Catal. Commun. 57 (2014) 99-102.
[43] M. Falorni, G. Giacomelli, A. Porcheddu, M. Taddei, The Journal of Organic Chemistry 64 (1999) 8962-8964.
[44] V.K. Sivasubramanian, M. Ganesan, S. Rajagopal, R. Ramaraj, The Journal of Organic Chemistry 67 (2002) 1506-1514.
[45] N. Hessenauer-Ilicheva, A. Franke, D. Meyer, W.-D. Woggon, R. van Eldik, J. Am. Chem. Soc. 129 (2007) 12473-12479.
[46] A.M. Aslam, S. Rajagopal, M. Vairamani, M. Ravikumar, Transition Met. Chem. 36 (2011) 751.
[47] Bruker, 2009, APEXII, Bruker AXS Inc., Madison, Wisconsin, USA,
[48] G.M. Sheldrick, AcCrA A64 (2008) 112-122.
[49] A. Altomare, M.C. Burla, M. Camalli, G.L. Cascarano, C. Giacovazzo, A. Guagliardi, A.G.G. Moliterni, G. Polidori, R. Spagna, Journal of Applied Crystallography 32 (1999) 115-119.

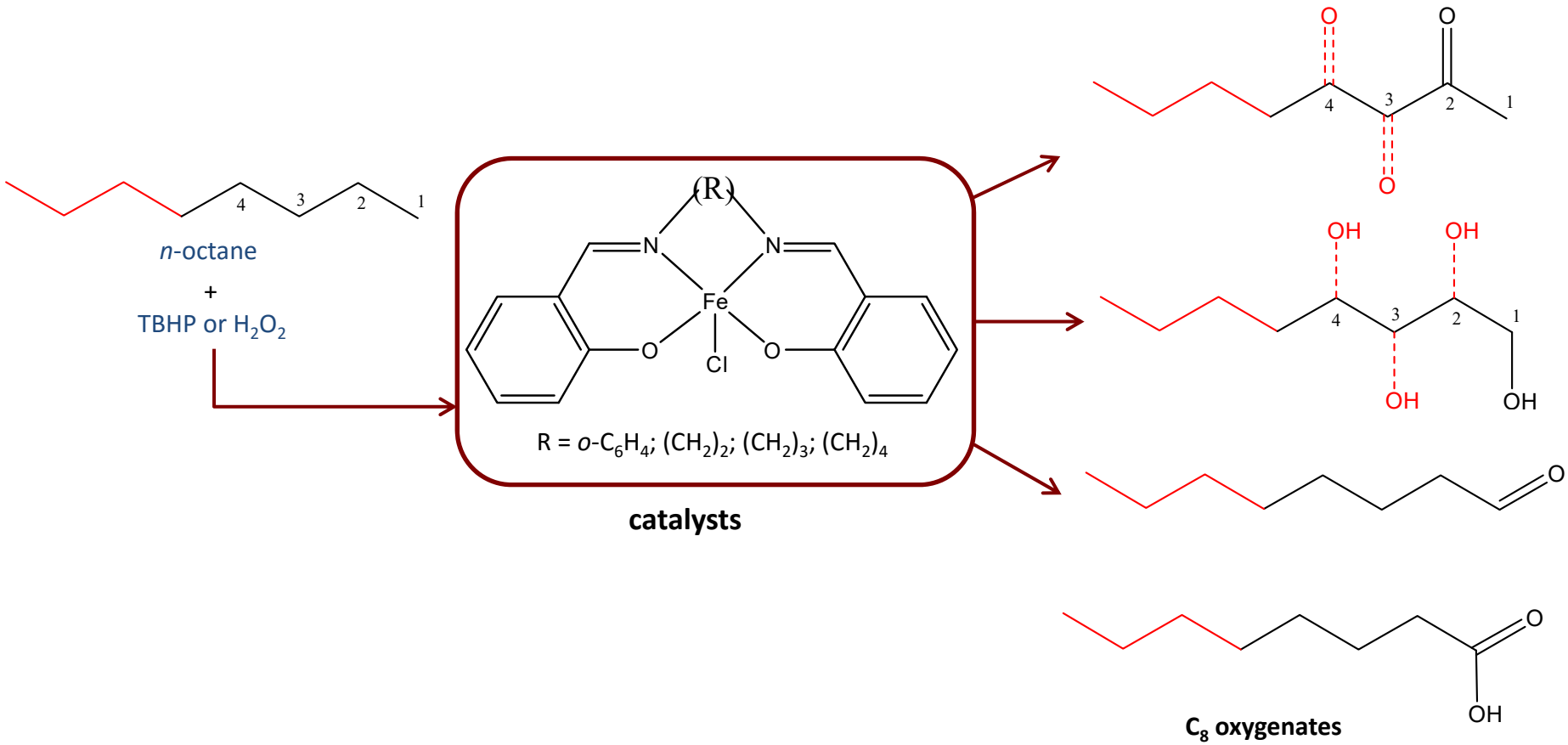

Highlights

Four salen-type iron complexes were prepared, each with a different ligand diamine bridging backbone.

Variation of the ligand backbone altered the electronics and sterics around the iron centres as observed by the use of IR spectroscopy and X-Ray crystallography.

All the complexes were found to be catalytically active in the oxidation of *n*-octane with H_2O_2 and TBHP as oxidants. The dominant product class was the ketones.